꙳ *Original Article* ꙳

Hemodynamic Simulation of Pancreaticoduodenal Artery Aneurysm Formation Using an Electronic Circuit Model and a Case Series Analysis

Kazuhiro Miyahara, MD,[1] Katsuyuki Hoshina, MD, PhD,[1] Jun Nitta, MD,[1]
Masaru Kimura, MD,[1] Sota Yamamoto, PhD,[2] and Marie Ohshima, PhD[3]

Objective: To assess mechanisms underlying aneurysm formation using a simple electronic circuit model.
Materials and Methods: We created a simple circuit model connecting the celiac artery (CA) to the superior mesenteric artery via the pancreaticoduodenal arcade. We retrospectively reviewed 12 patients with true pancreaticoduodenal artery aneurysms (PDAAs) who received open or endovascular treatment between 2004 and 2017. We set the resistance of each artery and organ voltage and calculated flow volume and rate in response to degrees of simulated CA stenosis from 0% to 99.9%.
Results: Flow volume rates of the anterior pancreaticoduodenal artery and posterior pancreaticoduodenal artery decreased to zero when CA stenosis increased from 0% to 50% and then increased drastically, at which point flow direction reverted and the flow was up to three times the initial rate. The gastroduodenal artery (GDA) also showed reversed flow with severe CA stenosis. In 12 patients with PDAA, eight presented with a CA lesion, and the other patients presented with comorbidities causing the arteries to be pathologically fragile, such as Marfan syndrome,

Behçet's disease, and segmental arterial mediolysis. All four GDA aneurysms were not accompanied by CA lesions.
Conclusion: The mechanism underlying CA-lesion-associated PDAA formation may be partially explained using our model.

Introduction

An arterial aneurysm is known to have a potential risk of rupture, and the rupture mechanism could be compared to a balloon that expands and bursts. Although there is evidence, especially with regard to aortic aneurysms, that multiple factors lead to rupture, including atherosclerotic change, distribution, inflammation, and saccular morphology, one of the most reliable and objective factors indicating the requirement for operative intervention is still the diameter of the aneurysm.[1,2] For most arterial aneurysms, the structural wall stress, rather than the hemodynamic stress, drives the arterial wall to deterioration and ultimately rupture.[3,4] However, a pancreaticoduodenal artery aneurysm (PDAA), which is a rare arterial aneurysm accounting for only 2% of all visceral artery aneurysms,[5,6] has two unique characteristics compared to other aneurysms. First, the rupture risk of PDAA is not related to its diameter.[7] Second, PDAA formation is closely associated with celiac artery (CA) stenosis or occlusion.[7–10] Researchers suggest that the pancreaticoduodenal artery (PDA) is influenced by hemodynamic changes, and the hypothesis that the CA lesion causes PDAA formation seems simple and understandable. However, the anatomy of the arcade is too complicated to create a simulation model; therefore, there are very few studies that have analyzed these phenomena. Herein, we created an electronic circuit model in which we could change the degree of CA stenosis and demonstrate the association with the flow in the PDA.

[1] *Division of Vascular Surgery, Department of Surgery, Graduate School of Medicine, The University of Tokyo, Tokyo, Japan*
[2] *Department of Mechanical Engineering, Graduate School, Shibaura Institute of Technology, Tokyo, Japan*
[3] *Interfaculty Initiative in Information Studies/Institute of Industrial Science, The University of Tokyo, Tokyo, Japan*

Then, we applied this model to 12 cases of PDAA at our institute.

Materials and Methods

Electronic circuit model

To create the electronic circuit model, we initially created a simple arcade from the celiac trunk to the superior mesenteric artery (SMA), which included the bifurcation passing the anterior and posterior sections of the pancreatic head (**Fig. 1**). To simplify the anatomical model, we created each lesion of the pancreaticoduodenal arcade, including the gastroduodenal artery (GDA), anterior pancreaticoduodenal artery (APDA), posterior pancreaticoduodenal artery (PPDA), and inferior pancreaticoduodenal artery (IPDA). The APDA and PPDA were connected in parallel. Next, we added the branches to the adjacent organs, including the liver, stomach, pancreas, and intestine, and the venous circulation was connected to an earth potential (**Fig. 2**).

We set the resistance of each lesion of the arcade. We used Poiseuille's law to calculate the fluid dynamics and compare to the Ohm's law relating to the electricity. Poiseuille's law is shown as the following equation:

$$Q = \frac{\pi}{8\eta} \cdot \frac{r^4}{l} \cdot \Delta P$$

$$\left(\begin{array}{l} Q: \text{flow, } \eta: \text{viscosity, } r: \text{radius,} \\ l: \text{length, } \Delta P: \text{pressure drop} \end{array} \right)$$

If the Q (flow) corresponded to the "I" in Ohm's law ($V = RI$: V: voltage, R: resistance, I: current), the vascular resistance (R) is in inverse proportion to the fourth power of the radius and in proportion to the vascular length.

We set the resistance of CA as $1\,\Omega$ and calculated the other resistances based on it. We recruited patients with no aneurysms and measured the diameter and length of each lesion with thin slice contrast-enhanced computed tomography (CT) images for use as controls (**Table 1**). We used these data to decide the rate of resistance of the arteries. We selected five patients with cancer for the control group, who were two men and three women aged 45 to 79 years (average: 65.8 years). Next, we referred to the physiological data of blood flow reported by Williams and Leggett[11] to decide the organ resistance with a circuit simulator (Circuit-Lab https://www.circuitlab.com) (**Fig. 2**). We omitted the capacitance, which should be nearly zero in steady flow, in this model to simplify the simulation because the purpose of the model was not to simulate case-specifically but to evaluate the trend of the flow change according to the degree of CA stenosis.

We changed the degree of CA stenosis from 0% to 99.9% and calculated the CA resistance, which changed from $1\,\Omega$ to $1.0 \times 10^{12}\,\Omega$ based on Poiseuille's law. We en-
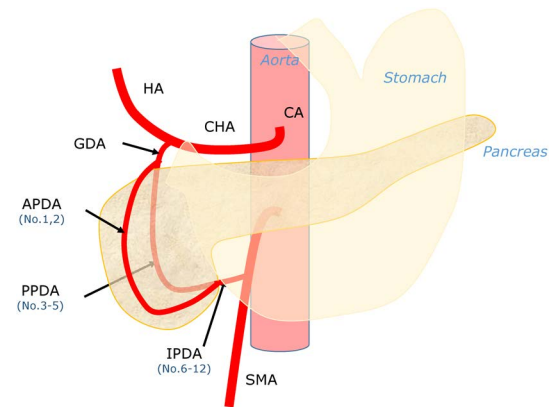

Fig. 1 Location of the posterior superior pancreaticoduodenal artery aneurysms.
HA: hepatic artery; CA: celiac artery; CHA: common hepatic artery; GDA: gastroduodenal artery; APDA: anterior pancreaticoduodenal artery; PPDA: posterior pancreaticoduodenal artery; IPDA: inferior pancreaticoduodenal artery; SMA: superior mesenteric artery

Fig. 2 The electronic circuit model of the pancreaticoduodenal arcade with the theoretical value of the resistance and the voltage.
CA: celiac artery; GDA: gastroduodenal artery; APDA: anterior pancreaticoduodenal artery; PPDA: posterior pancreaticoduodenal artery; IPDA: inferior pancreaticoduodenal artery; SMA: superior mesenteric artery
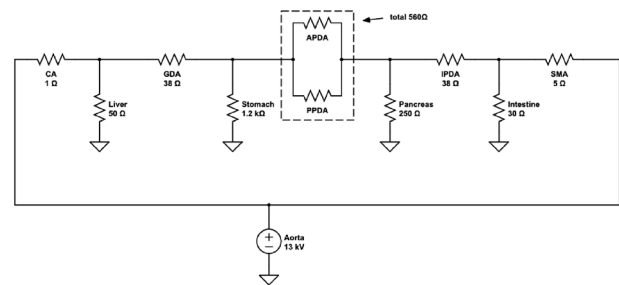
Table 1 The diameter and the length of the CA, SMA, and pancreaticoduodenal arcade arteries of a non-PDAA control group

	Diameter [mean±SD (mm)]	Length [mean±SD (mm)]
CA	6.35±0.69	22.52±2.49
GDA	2.89±0.43	29.62±5.77
APDA	1.34±0.17	71.22±21.13
PPDA	1.45±0.14	52.74±20.26
IPDA	2.50±0.93	20.89±9.18
SMA	5.51±1.09	63.90±22.57

CA: celiac artery; SMA: superior mesenteric; PDAA: posterior superior pancreaticoduodenal artery aneurysm; GDA: gastroduodenal artery; APDA: anterior pancreaticoduodenal artery; PPDA: posterior pancreaticoduodenal artery; IPDA: inferior pancreaticoduodenal artery; SD: standard deviation

Table 2 Characteristics of the 12 cases of PDAA

No.	Location	Concomitant disease	Age/sex	CA lesion	CA stenosis (%)	Diameter (mm)	Morphology
1	APDA		72/M	Occlusion	100	14	Saccular
2	APDA		62/M	Stenosis	68	10	Saccular
3	PPDA		46/F	Stenosis	71	N/A	Ruptured
4	PPDA		79/F	Stenosis	56	6	Fusiform
5	PPDA (multiple)	Marfan	42/F	Intact	0	N/A	Ruptured
6	APDA, PPDA	SAM	61/F	Intact	0	N/A	Ruptured
7	IPDA		55/F	Stenosis	74	12	Saccular
8	IPDA		40/M	Stenosis	61	21	Saccular
9	IPDA		48/F	Occlusion	100	10	Saccular
10	IPDA		58/F	Occlusion	100	28	Fusiform
11	IPDA	Behçet's disease	47/M	Intact	0	17	Fusiform
12	IPDA (multiple)	SAM	76/M	Intact	0	N/A	Ruptured
#1	GDA		76/F	Intact	0	12	Saccular
#2	GDA		55/F	Intact	0	7	Saccular
#3	GDA		66/F	Intact	0	6	Saccular
#4	GDA		81/F	Intact	0	4	Saccular

PDAA: pancreaticoduodenal artery aneurysm; CA: celiac artery; APDA: anterior pancreaticoduodenal artery; PPDA: posterior pancreatico-duodenal artery; IPDA: inferior pancreaticoduodenal artery; GDA: gastroduodenal artery; SAM: segmental arterial mediolysis

tered these values into the circuit simulator and calculated the hypothetical blood flow volume.

Patients

We retrospectively reviewed 12 patients with true PDAA who received open or endovascular treatment in our department between 2004 and 2017 (**Table 2**). The aneurysms were classified according to the location: APDA, PPDA, or IPDA (**Fig. 1**). Five patients with aneurysms were men and seven were women. The average age was 57.1 ± 13.2 years. The shape of the aneurysm was saccular in five patients and fusiform in three patients, and four patients presented with ruptured aneurysms whose morphology could not be evaluated. We diagnosed these patients as having a true aneurysm because they did not have pancreatitis, aortic dissection, or a history of trauma. To exclude the pancreatitis, we checked the level of serum amylase.

For collecting data on normal arterial geometry (diameter and length), we selected five patients with cancer and no aneurysms who were admitted to our hospital and measured their arterial geometry using thin sliced CT images. The use of the imaging data for the research was approved by the Ethics Committee of The University of Tokyo Hospital (No. 3316-(3), 3252-(5)) and all patients provided written informed consent.

Statistical analysis

Intra-group differences were compared using a Mann–Whitney's U-test for continuous variables. Values are reported as a mean ± standard deviation. The statistical significance was set at p < .05.

Results

Changes in the hypothetical blood flow in response to CA stenosis

We referred to the average human blood flow values introduced in the review article by Williams and Leggett[11] to set the voltage of the organs in our electrical circuit model. The distribution of the blood flow volume was 6.5% of the cardiac output for the hepatic artery, 12.5% for the intestines, 1% for the pancreas, and 1% for the stomach. As blood is supplied to the stomach from four main arteries (right gastric, left gastric, right epiploic, and left epiploic artery), we simply set the outflow toward the stomach by dividing 1% by four (that is, 0.25% of the cardiac output). We set the resistance of the arteries via Ohm's law with the arterial diameter and length of the data derived from the five patients without aneurysms (**Table 1**). To understand the circuit model easily and intuitively, we arbitrarily assigned the following concrete values: voltage of the aorta was 13 kV, which was derived from $13 \, \text{hPa} \approx 100 \, \text{mmHg}$ of the average blood pressure, and the cardiac output was 5,000 mL/min (**Fig. 2**).

According to average human data,[11] we set the default blood flow volume values (Q) under the intact CA as 401 mL/min for the SMA, 14.6 mL/min for the GDA, 269 mL/min for the CA, 34.3 mL/min for the IPDA, and 14.6 mL/min for the APDA or the PPDA. The flow volume ratio (QR) in response to CA stenosis was calculated according to the following equation: Q divided by Q without CA stenosis. In response to CA stenosis, Q or the SMA and PPDA increased, the CA decreased at an accelerated rate at around 50% stenosis, and the GDA, APDA, and
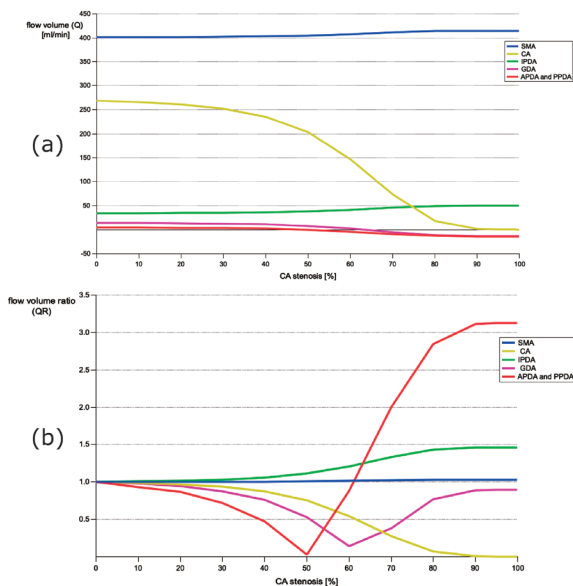
Fig. 3 (**a**) Change of the flow volume with the degree of celiac artery stenosis; (**b**) Change of the flow volume ratio with the degree of celiac artery stenosis.
CA: celiac artery; SMA: superior mesenteric artery; IPDA: inferior pancreaticoduodenal artery; GDA: gastroduodenal artery; APDA: anterior pancreaticoduodenal artery

IPDA decreased and reverted at 60% and 50% stenosis, respectively (**Fig. 3a**). In **Fig. 3b**, the flow changes in the GDA, APDA, and PPDA from antegrade to retrograde were well demonstrated. The absolute value of the retrograde flow volume of the APDA and PPDA became three times that of the antegrade flow volume. The shape of the GDA flow inverted symmetrically at 60% CA stenosis. The QRs of the pancreatoduodenal arcade (APDA, PPDA, and IPDA) were positive under severe CA stenosis, which was different to other arteries (**Fig. 3b**).

Application of the simulation data to patients with PDAA

Among the 12 patients with PDAA, eight without concomitant systemic disease had CA stenosis. These patients had more than 50% CA stenosis, and six patients had CA stenosis over 65%, in which the QR rapidly increased. One patient had Behçet's disease, one patient had Marfan's syndrome, and two patients had clinically diagnosed segmental arterial mediolysis (SAM). None of these patients had a CA lesion. There were also no CA lesions in any of the four patients with GDA aneurysms (**Table 2**).

We compared the age of patients with PDAA and patients with GDA to evaluate the atherosclerotic contribution in this cohort. The mean age of the four patients with GDA was higher than that of the patients with PDAA (69.5 ± 11.5 vs. 57.1 ± 13.2 years), but the difference was not significant ($p = .129$).

Discussion

Our electric circuit model is simple and adequately replicates the route between the CA and SMA for simulating the hemodynamic changes in response to CA stenosis.

The association between PDAA formation and CA lesions was first reported by Sutton and Lawton.[12] They suggested that the possible mechanism of increased collateral flow of the pancreaticoduodenal arcade was due to the decreased flow from the CA to the PDAA. This explanation has been widely accepted and seems plausible despite not being supported by evidence, most likely because PDAA is very rare and, therefore, impossible to analyze in a large sample, and the arterial anatomy of the arcade is too complicated.[13]

An interesting finding was that the flow volume of the APDA and the PPDA changed drastically. The flow volume decreased until the stenosis progressed up to 50%; thereafter, it increased up to three times that of the initial volume with retrograde flow. This drastic hemodynamic change in the artery influences the PDA and might cause PDAA formation. Interestingly, patients with PDAA without concomitant disease in our case series showed severe CA stenosis, which might confirm the result obtained from the simulation in our model.

In our study, we showed that the simulated blood flow was a suitable hemodynamic parameter for assessing the changes in flow because it is proportional to the shear stress according to the Hagen–Poiseuille law,

$$\tau = \frac{4\mu}{\pi} \cdot \frac{Q}{r^3}$$

$$\left(\begin{array}{l} \tau\text{: wall shear stress, } \mu\text{: coefficient of friction,} \\ r\text{: radius, } Q\text{: flow} \end{array} \right)$$

under the laminar flow and without a diameter change. However, oscillatory flow and the arterial enlargement due to the remodeling should be included in the model to assess the mechanism of aneurysm formation. In the hemodynamic and biological pathway of intracranial aneurysms hypothesized by Meng et al.,[14] a small, thin-wall, and non-atherosclerotic aneurysm was triggered by high wall shear stress (WSS) combined with a positive WSS gradient. Considering the specific PDA findings demonstrated in our study, PDAA might be on the pathway.

Mano et al. measured parameters including flow volume and WSS with four-dimensional flow-sensitive magnetic resonance imaging and demonstrated the retrograde flow in the GDA, similar to our result.[15] They also showed the flow with a heterogeneous distribution of low WSS and a high oscillatory shear index in the PDA and speculated that these parameters might be associated with aneurysm formation.[15] However, as the CA was occluded in all five cases, their case-specific analysis only demonstrated the

hemodynamic condition at one time point, which could not reflect the WSS gradient responding to CA stenosis, unlike our model.[15]

In clinical application, this model has one major limitation—the anatomical variation of the pancreaticoduodenal arcade. A missing arcade and the loss of anastomosis between the IPDA and APDA and PPDA have been previously reported to make clinical application difficult.[13] However, the parallel setting of the APDA and PPDA could represent the real-life wide variations in the complicated parapancreatic artery. In addition, most of the PDAAs without a missing arcade should be categorized as one of three types (APDA, PPDA, or IPDA) when considering the inflow and outflow of the aneurysms through the CA to the SMA in the model. For example, one aneurysm (No. 7, **Table 2**) was located on the transverse pancreatic artery. As this aneurysm formed a shunt connecting the anterior arcade to the SMA,[13] we categorized it as an IPDA. We assumed that such a categorization should not influence the simulation of the hemodynamic changes. Ideally, assembling each electronic circuit specific to each case in the future is necessary.

We initially assumed that the GDA was also influenced by the hemodynamic change; however, no GDA aneurysms were accompanied by a CA lesion in our series. Vandy et al. reviewed the previous reports on PDAA and GDA aneurysms with CA lesions and found 105 PDAAs and only 10 GDA aneurysms.[16] Considering the distribution of these aneurysms in splanchnic artery aneurysms—4% for GDA aneurysms and 9% for PDAAs[17]—this indicates that the PDA is more frequently associated with CA lesions than the GDA. In our results, the flow of GDA changed its direction at 60% CA stenosis, which might contribute to aneurysm formation. A relatively low QR might be one of the reasons why the GDA hemodynamics were not as strongly affected. In addition, patients with GDA aneurysms were older than patients with PDAA, although the difference was not significant. Atherosclerotic changes in the arterial wall of the GDA might be another reason.

Tissue fragility that results from comorbid diseases may also cause PDAA. Therefore, we may attribute aneurysm formation in patients with Behçet's disease, Marfan syndrome, and SAM to the fragile arterial wall. Two patients with multiple splanchnic artery aneurysms were clinically diagnosed with SAM based on radiological features (string of beads appearance) and a non-atherosclerotic and non-inflammatory background. In case No. 6, a new aneurysm emerged after the coil embolization for the initial aneurysm and remodeling represented the specific "acute" feature of SAM.[18,19] As this tissue disorder should ideally be diagnosed based on pathological results, PDA patients with SAM or fibromuscular dysplasia may have

potentially existed. We should suspect a comorbid disease when we come across patients with PDAA without CA lesions or when aneurysms emerge in succession.

Two major causes of CA stenosis or occlusion are compression by the median arcuate ligament and atherosclerotic changes. Surgical interventions such as ligament resection, endovascular stent insertion, or bypass surgery may be performed. Whether or not intervention for the CA lesion should be performed after treatment of the PDAA remains controversial.[7,20–22] The current literature reports very few cases of recurrence of PDAA in the long term.[23–25] We assumed, from our simulation, that chronological hemodynamic changes initiate aneurysm formation, and once the aneurysm is treated, the pancreaticoduodenal arcade becomes hemodynamically stable and additional intervention for the CA lesion would be unnecessary.

Conclusion

We created an electronic circuit model of the pancreaticoduodenal arcade and demonstrated the flow volume changes in response to CA stenosis. The flow of the APDA and PPDA reverted and increased drastically with severe stenosis. Clinically, patients with PDAA without tissue fragility also had CA lesions, but patients with GDA did not. Our model may be helpful for further assessment of the mechanism underlying PDAA formation.

Funding

Disclosure Statement

There is no conflict of interest to declare.

Author Contributions

Study conception: KH
Data collection: KH, JN, MK
Data analysis: MK
Analysis: SY
Investigation: KH, MO
Writing: KM
Critical review and revision: all authors
Final approval of the article: all authors
Accountability for all aspects of the work: all authors

References

1) Choke E, Cockerill G, Wilson WRW, et al. A review of biological factors implicated in abdominal aortic aneurysm rupture. Eur J Vasc Endovasc Surg 2005; **30**: 227-44.

2) JCS Joint Working Group. Guidelines for diagnosis and treatment of aortic aneurysm and aortic dissection (JCS 2011). Circ J 2013; **77**: 789-828.

3) Akai T, Hoshina K, Yamamoto S, et al. Biomechanical analysis of an aortic aneurysm model and its clinical application to thoracic aortic aneurysms for defining "saccular" aneurysms. J Am Heart Assoc 2015; **4**: e001547.

4) Humphrey JD, Holzapfel GA. Mechanics, mechanobiology, and modeling of human abdominal aorta and aneurysms. J Biomech 2012; **45**: 805-14.

5) Paty PSK, Cordero JA Jr, Darling RC 3rd, et al. Aneurysms of the pancreaticoduodenal artery. J Vasc Surg 1996; **23**: 710-3.

6) Stanley JC, Wakefield TW, Graham LM, et al. Clinical importance and management of splanchnic artery aneurysms. J Vasc Surg 1986; **3**: 836-40.

7) Ducasse E, Roy F, Chevalier J, et al. Aneurysms of the pancreaticoduodenal arteries with celiac trunk lesion: current management. J Vasc Surg 2004; **39**: 906-11.

8) de Perrot M, Berney T, Deléaval J, et al. Management of true aneurysms of the pancreaticoduodenal arteries. Ann Surg 1999; **229**: 416-20.

9) Ritter JC, Johnston M, Caruana MF, et al. Aorto-gastroduodenal bypass grafting for an inferior pancreaticoduodenal aneurysm and celiac trunk thrombosis. Interact Cardiovasc Thorac Surg 2010; **10**: 125-7.

10) Nishiyama A, Hoshina K, Hosaka A, et al. Treatment strategies for a pancreaticoduodenal artery aneurysm with or without a celiac trunk occlusive lesion. Ann Vasc Dis 2013; **6**: 725-9.

11) Williams LR, Leggett RW. Reference values for resting blood flow to organs of man. Clin Phys Physiol Meas 1989; **10**: 187-217.

12) Sutton D, Lawton G. Coeliac stenosis or occlusion with aneurysm of the collateral supply. Clin Radiol 1973; **24**: 49-53.

13) Murakami G, Hirata K, Takamuro T, et al. Vascular anatomy of the pancreaticoduodenal region: a review. J Hepatobiliary Pancreat Surg 1999; **6**: 55-68.

14) Meng H, Tutino VM, Xiang J, et al. High WSS or low WSS? Complex interactions of hemodynamics with intracranial aneurysm initiation, growth, and rupture: toward a unifying hypothesis. AJNR Am J Neuroradiol 2014; **35**: 1254-62.

15) Mano Y, Takehara Y, Sakaguchi T, et al. Hemodynamic assessment of celiaco-mesenteric anastomosis in patients with pancreaticoduodenal artery aneurysm concomitant with celiac artery occlusion using flow-sensitive four-dimensional magnetic resonance imaging. Eur J Vasc Endovasc Surg 2013; **46**: 321-8.

16) Vandy FC, Sell KA, Eliason JL, et al. Pancreaticoduodenal and gastroduodenal artery aneurysms associated with celiac artery occlusive disease. Ann Vasc Surg 2017; **41**: 32-40.

17) Corey MR, Ergul EA, Cambria RP, et al. The natural history of splanchnic artery aneurysms and outcomes after operative intervention. J Vasc Surg 2016; **63**: 949-57.

18) Slavin RE. Segmental arterial mediolysis: course, sequelae, prognosis, and pathologic-radiologic correlation. Cardiovasc Pathol 2009; **18**: 352-60.

19) Nishikawa Y, Hoshina K, Sasaki H, et al. Acute remodeling of an adjoining aneurysm after endovascular treatment of a ruptured splanchnic arterial aneurysm: a case of clinically diagnosed segmental arterial mediolysis. Ann Vasc Dis 2012; **5**: 449-53.

20) Tarazov PG, Ignashov AM, Pavlovskij AV, et al. Pancreaticoduodenal artery aneurysm associated with celiac axis stenosis. Dig Dis Sci 2001; **46**: 1232-5.

21) Boll JM, Sharp KW, Garrard CL, et al. Does management of true aneurysms of peripancreatic arteries require repair of associated celiac artery stenosis? J Am Coll Surg 2017; **224**: 199-203.

22) El-Hayek KM, Titus J, Bui A, et al. Laparoscopic median arcuate ligament release: are we improving symptoms? J Am Coll Surg 2013; **216**: 272-9.

23) Brocker JA, Maher JL, Smith RW. True pancreaticoduodenal aneurysms with celiac stenosis or occlusion. Am J Surg 2012; **204**: 762-8.

24) Waldenberger P, Bendix N, Petersen J, et al. Clinical outcome of endovascular therapeutic occlusion of the celiac artery. J Vasc Surg 2007; **46**: 655-61.

25) Pulli R, Dorigo W, Troisi N, et al. Surgical treatment of visceral artery aneurysms: a 25-year experience. J Vasc Surg 2008; **48**: 334-42.